# Optimal Compensation of Dual Carrier Frequency Offsets for MISO-mode DVB-T2

**Eun-Sung Jeon[1], Jeong-Wook Seo[2], Jang-Hoon Yang[3], Jong-Ho Paik[4] and Dong-Ku Kim[1]**
[1] Department of Electrical and Electronic Engineering, Yonsei University
134 Sichon-dong, Seodaemun-gu, Seoul 120-749, Korea
[e-mail: youngmil2@yonsei.ac.kr, dkkim@yonsei.ac.kr]
[2] Advanced Mobile Technology Research Center, Korea Electronic Technology Institute
1599 Sangam-dong, Mapo-gu, Seoul 121-835, Korea
[e-mail: jwseo@keti.re.kr]
[3] Deparment of Newmedia, Korea German Institute of Technology
661 Deungchon-dong, Kangseo-gu, Seoul 157-030, Korea
[e-mail: jhyang@kgit.ac.kr]
[4] Multimedia Department, Seoul Women's University,
621 Hwarang-ro, Nowon-gu, Seoul 139-774, Korea
[e-mail: paikjh@swu.ac.kr]
*Corresponding author: Dong-Ku Kim

*Received October 11, 2011; revised December 30, 2011; accepted January 26, 2012; published February 28, 2012*

## *Abstract*

Dual carrier frequency offsets (CFOs) occur in multiple-input single-output (MISO)-mode DVB-T2 systems, where signals are transmitted simultaneously from two *distributed* transmitters in a single frequency network (SFN). In this paper, we first derive an optimal compensation frequency for dual CFOs. We also propose an algorithm that optimizes the compensation frequency for the MISO-mode DVB-T2 application. Its performance is compared with the conventional scheme by using a full DVB-T2 simulator.

***Keywords:*** DVB-T2, MISO, OFDM, carrier frequency offset.

**DOI: 10.3837/tiis.2012.02.010**

## 1. Introduction

DVB-T2 is the next-generation European terrestrial digital broadcasting standard that was published by the European Telecommunication Standard Institute (ETSI) in 2008 [1]. Currently, several European countries such as the United Kingdom, Finland, and Sweden are launching digital high definition television (HDTV) services using DVB-T2. It is expected that many other countries deploying its predecessor, DVB-T, will update their standard to DVB-T2 with the approach of Analogue Switch-Off (ASO). Some of the commercial requirements that have acted as a framework for the T2 development are as follows: (1) T2 should provide improved single-frequency network (SFN) performance compared with DVB-T and (2) T2 transmissions must be able to reuse existing domestic receive antenna installations and existing transmitter infrastructures [2]. (This requirement ruled out the consideration of multiple-input multiple-output (MIMO) techniques that would involve both new receiver and transmit antennas.) To meet these commercial requirements, T2 incorporates the option of the multiple-input single-output (MISO) mode using the Alamouti transmit-diversity technique [3], in which the second remote transmitter transmits a slightly modified version of each pair of data subcarriers in reverse order as shown in **Fig. 1**. According to [3], this technique gives the same diversity gain as the reception with two receive antennas and results in around 15 dB gain in the signal-to-noise ratio (SNR) at a bit error rate (BER) of $10^{-4}$ in uncoded binary phase-shift keying (BPSK) systems.

As with DVB-T, DVB-T2 uses an orthogonal frequency division multiplex (OFDM) modulation. The performance of OFDM is sensitive to the carrier frequency offset (CFO) since the CFO breaks the orthogonality between subcarriers, which results in inter-carrier interference (ICI) from other subcarriers. CFO occurs mainly due to the frequency mismatch between oscillators in the transmitter and the receiver. For example, if the accuracy of the oscillator is 10 parts per million (PPM) and the carrier frequency of the DVB-T2 signal is 800 MHz, a maximum CFO of 8-KHz is caused by the mismatched oscillators. There have been many literatures dealing with CFO synchronization technique in OFDM systems [4][5][6]. In DVB-T2, a special preamble symbol named the P1 symbol is defined for the initial estimate of the CFO. As shown in **Fig. 2**, the P1 symbol is inserted at the beginning of every DVB-T2 frame with guard intervals at both ends; these are frequency-shifted repetitions of the main part of the P1 symbol. This structure can be exploited for increasing the correlation between the main part of the P1 symbol and the two intervals. At the receiver, the CFO is estimated by taking the argument of correlator output's peak during the P1 symbol decoding process.

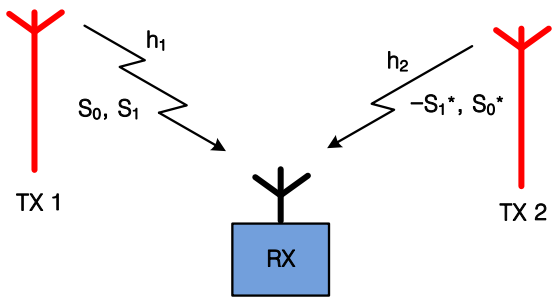


**Fig. 1.** MISO scheme [1]

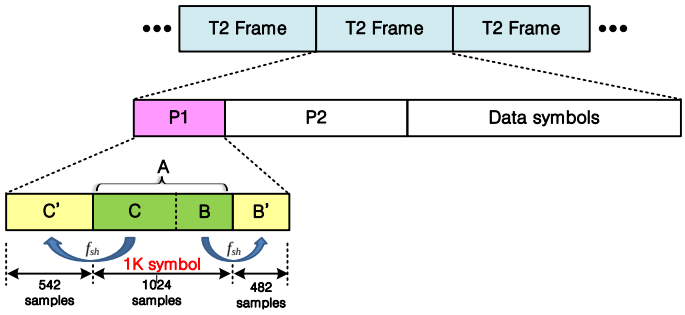


**Fig. 2.** P1 symbol structure [1]

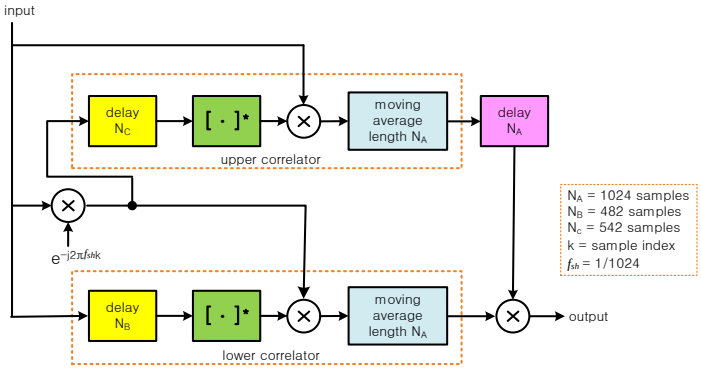


**Fig. 3.** Block diagram of P1 correlator [2]

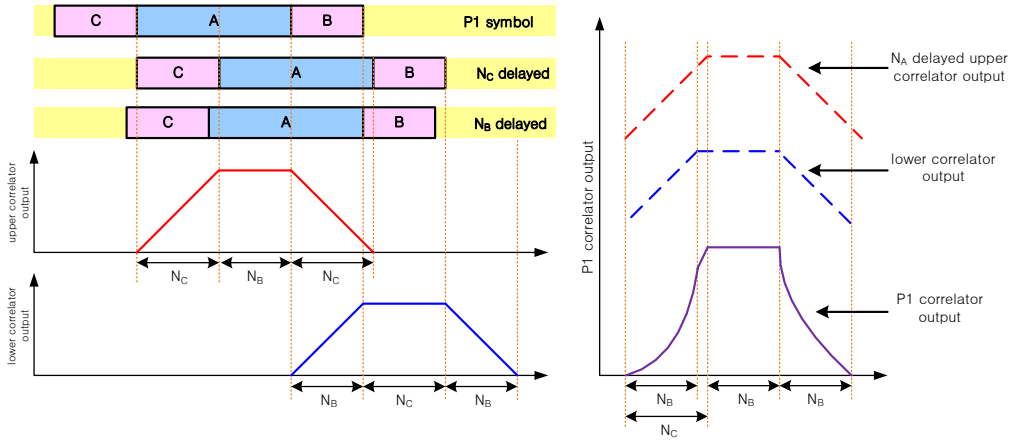


**Fig. 4**. Output pulse of P1 correlator [2]

In [2], the implementation of P1 symbol correlation scheme to estimate the CFO was suggested as shown in **Fig. 3**. The resulting output pulse is shown in **Fig. 4**. If a suitable threshold is applied, the estimate of the CFO can be obtained by taking the argument of middle point between the first sample and the last sample which exceed the threshold.

If DVB-T2 uses the MISO-mode where signals are transmitted simultaneously from two spatially separated transmitters with their own oscillators, two distinct CFOs, i.e., dual CFOs, may exist in the received signal, one for each transmitter. Recently, various studies have been

conducted on multiple CFOs [7][8][9][10][11][12][13][14[15][16]. These can be classified into two main topics:

- Estimation of multiple CFOs: Oh *et al.* [7] designed pilot patterns that separate each transmitter-receiver link in a time division multiple access (TDMA) fashion to provide decoupled CFOs. For similar reasons, Huang *et al.* [8] proposed a training sequence consisting of several groups of contiguous subcarriers in the frequency domain that are assigned to each transmitter, which is similar to downlink orthogonal frequency division multiple access (OFDMA). Non-pilot-aided estimation of multiple CFOs was suggested in [9], where it was required that the delay of received signals should be randomly distributed. Multiple CFOs estimation methods for point-to-point MIMO systems were presented in [10] and [11]. However, the conventional multiple CFOs estimation methods cannot be directly applied to the DVB-T2 due to the use of different training sequences.
- Equalization techniques to mitigate ICI caused by multiple CFOs: A frequency domain equalizer was proposed in [12] where the off-diagonal elements of the frequency domain channel matrix corresponding to the ICI are eliminated; this is similar to ICI cancellation for a single-input single-output (SISO) OFDM system. However, this approach suffers from performance loss in the high SNR region. In order to remove the error floor, an iterative decoding technique was proposed in [13], where the ICI terms in the channel matrix are gradually eliminated by iterations at the cost of increased complexity. In [14], time domain equalization using the Viterbi algorithm was proposed. Further research on equalization to both improve performance and reduce complexity has been reported in [15] and [16]. Such studies related to this topic have assumed that all CFOs are perfectly estimated at the receiver.

In MISO-mode DVB-T2, the P1 correlator provides a *single* CFO estimate by processing the sum of two concurrently received P1 symbols. Thus, it is impossible for the MISO-mode DVB-T2 system to simultaneously estimate the dual CFOs. Furthermore, even though the dual CFOs are compensated by using this CFO estimate, there always remains ICI. We call such ICI *residual ICI*. Our conjecture is that there may exist an optimal compensation frequency that minimizes the power of residual ICI. So far, little attention has been paid to this problem, and to the best of our knowledge, no results on this problem have been established. This paper presents an optimal compensation frequency that minimizes the power of residual ICI for two MISO scenarios in the implementation guideline [2]: both paths have nearly the same attenuation and the two paths have different attenuations. We first derive an optimal solution under the assumption that perfect estimates of dual CFOs are given to the receiver. Next, we propose an algorithm that adjusts the initial compensation frequency obtained from the P1 correlator to the optimal solution without requiring estimates of dual CFOs.

The rest of this paper is organized as follows. In Section 2, the system model is presented and the optimal compensation frequency is derived. In Section 3, the algorithm for finding the optimal compensation frequency is proposed. The numerical results are presented in Section 4, and finally, the conclusions are given in Section 5.

## 2. Analysis on Optimal Compensation Frequency for Dual Carrier Frequency Offsets

### 2.1 System Model

Let us consider two separate transmitters in a SFN sending signals to a receiver. A time domain transmitted OFDM signal excluding P1 symbol from each transmitter can be expressed as

$$x_n(t) = \sum_{k=0}^{N-1} X_{k,n} e^{j2\pi f_k t}, \quad -T_g \le t \le T_s, \tag{1}$$

where $X_{k,n}$, $k = 1, \ldots, N$, $n = 1, 2$, is the Alamouti-encoded data (or a pilot) for subcarrier $k$ in the $n$-th transmitter. $N$ and $T_s$ denote the number of subcarriers and the duration of one OFDM symbol, respectively and $f_k$ is the $k$-th subcarrier frequency. $T_g$ is the duration of cyclic prefix (CP). Alamouti encoding is applied in space and frequency (space-frequency coding). For example, if a pair of data ($X_0$, $X_1$) is coming from the output of the frequency interleaver, then a pair of unmodified data ($X_0$, $X_1$) is directed to transmitter 1 and a pair of modified data ($-X_1^*$, $X_0^*$) is conveyed to transmitter 2.

Pilots—P2 pilots, scatter pilots, continual pilots, edge pilots, and frame closing pilots—are inserted into OFDM symbols at regular intervals in time and frequency directions. To be specific, P2 pilots, which have a relatively dense pilot pattern, are inserted on every third subcarrier in P2 symbols (preambles) that carry L1 signaling [2]. Scatter pilots are defined by eight patterns (PP1–PP8) and are inserted in data symbols. **Fig. 5** illustrates each of the pilots where PP3 is adopted for scatter pilots. (This pattern will be adopted in our simulation that is presented in Section 4.) Here, parameters $D_x$ and $D_y$ are the distances of pilot-bearing subcarriers in frequency and time, respectively.

Then, the received signal with dual CFOs can be written as

$$y(t) = e^{j2\pi\varepsilon_1 t} \sum_{l=0}^{L_1-1} h_1(l) x_1(m-l) + e^{j2\pi\varepsilon_2 t} \sum_{l=0}^{L_2-1} h_2(l) x_2(m-l) + n(t), \tag{2}$$

where $\varepsilon_n$ is the CFO between the receiver and $n$-th transmitter and $n(t)$ is additive white Gaussian noise (AWGN). $h_n(l)$ denotes the channel impulse response of the $l$-th tap, $l \in \{0, \ldots, L_n\text{-}1\}$, and $L_n$ is the number of channel taps. Here we assume that CP duration $T_g$ is longer than the maximum channel delay spread for both channel, i.e., $T_g \ge \max(L_1, L_2)$. We also assume that the channel is a quasi-static fading channel, i.e., channel taps do not change during one OFDM symbol, and vary independently from one OFDM symbol to another. After sampling at $t = mT_s/N$, where $m$ is a sample index ($0 \le m \le N\text{-}1$), (2) can be written as

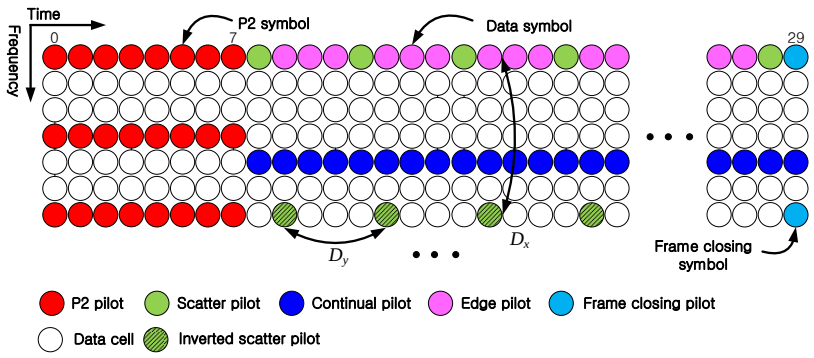


**Fig. 5.** MISO pilot arrangement (PP3 for scatter pilot) [1]

$$\begin{aligned} & y(mT_s/N) \equiv y[m] \\ & = e^{j2\pi f_f^{(1)}\frac{m}{N}}\sum_{l=0}^{L_1-1} h_1[l]x_1[m-l] + e^{j2\pi f_f^{(2)}\frac{m}{N}}\sum_{l=0}^{L_2-1} h_2[l]x_2[m-l] + n[m], \end{aligned} \tag{3}$$

where $f_f^{(n)} = \varepsilon_n T_s$ is the CFO normalized by the symbol rate. We assume that normalized CFOs are in the range of half the symbol rate, i.e., -0.5 $\leq f_f^{(n)} \leq$ 0.5 for $n$ = 1, 2. Let $f_c$ denote the estimate of CFO obtained from a P1 correlator. After compensating the dual CFOs with $f_c$, we have

$$\begin{aligned} & y[m]e^{\frac{-j2\pi f_c m}{N}} \equiv \tilde{y}[m] \\ & = e^{j2\pi\left(f_f^{(1)}-f_c\right)\frac{m}{N}}\sum_{l=0}^{L_1-1} h_1[l]x_1[m-l] + e^{j2\pi\left(f_f^{(2)}-f_c\right)\frac{m}{N}}\sum_{l=0}^{L_2-1} h_2[l]x_2[m-l] + \tilde{n}[m]. \end{aligned} \tag{4}$$

After CP removal and subsequent fast Fourier transform (FFT), we get

$$\begin{aligned} Y_p &= \frac{1}{N}\sum_{m=0}^{N-1}\tilde{y}[m]e^{\frac{-j2\pi pm}{N}} \\ &= \sum_{k=0}^{N-1} X_{k,1}H_{k,1}\Lambda_{k,p}^{(1)} + \sum_{k=0}^{N-1} X_{k,2}H_{k,2}\Lambda_{k,p}^{(2)} + N_p, \end{aligned} \tag{5}$$

where $H_{k,n}$, is channel frequency response, $N_p$ is AWGN on the $p$-th subcarrier and

$$\begin{aligned} \Lambda_{k,p}^{(n)} &= \frac{1}{N}\sum_{m=0}^{N-1} e^{j2\pi\left(k+(f_f^{(n)}-f_c)-p\right)\frac{m}{N}} \\ &= e^{j\pi\left(k+(f_f^{(n)}-f_c)-p\right)\frac{N-1}{N}} \cdot \frac{\sin\left(\pi(k+(f_f^{(n)}-f_c)-p)\right)}{N\sin\left(\pi(k+(f_f^{(n)}-f_c)-p)/N\right)}. \end{aligned} \tag{6}$$

Let {($X_{p,1}$, $X_{p+1,1}$), ($X_{p,2}$, $X_{p+1,2}$)} be an Alamouti coding block, i.e., $X_{p,2} = -X_{p+1,1}^*$ and $X_{p+1,2} = X_{p,1}^*$. We can then decompose (5) as

$$Y_p = X_{p,1}H_{p,1}\Lambda_{p,p}^{(1)} - X_{p+1,1}^* H_{p,2}\Lambda_{p,p}^{(2)} + \sum_{k=0,k\neq p}^{N-1} X_{k,1}H_{k,1}\Lambda_{k,p}^{(1)} + \sum_{k=0,k\neq p}^{N-1} X_{k,2}H_{k,2}\Lambda_{k,p}^{(2)} + N_p, \tag{7}$$

where the first two terms on the right-hand side are the desired signal and the remaining terms denote ICI and noise. Thus, dual CFOs always contain residual ICI, no matter how the CFO compensation is utilized.

### 2.2 Finding the Optimal Compensation Frequency

Our first goal is to find the optimal value of the compensation frequency $f_c$ that minimizes the effect of residual ICI. For that, we used the power of the residual ICI-plus-noise as an objective function. Given the normalized CFOs for $n$ = 1, 2, the objective function can be written as a

function of a single variable $f_c$ as

$$\begin{aligned} J_p(f_c) &= E\left\{\left|\sum_{\substack{k=0,\\k\neq p}}^{N-1} X_{k,1}H_{k,1}\Lambda_{k,p}^{(1)} + \sum_{\substack{k=0,\\k\neq p}}^{N-1} X_{k,2}H_{k,2}\Lambda_{k,p}^{(2)} + N_p\right|^2\right\} \\ &= E\left\{\left|\sum_{\substack{k=0,\\k\neq p}}^{N-1} X_{k,1}H_{k,1}\Lambda_{k,p}^{(1)}\right|^2\right\} + E\left\{\left|\sum_{\substack{k=0,\\k\neq p}}^{N-1} X_{k,2}H_{k,2}\Lambda_{k,p}^{(2)}\right|^2\right\} + E\left\{\left|N_p\right|^2\right\} \\ &= \sigma_{H,1}^2 S_p(f_f^{(1)} - f_c) + \sigma_{H,2}^2 S_p(f_f^{(2)} - f_c) + \sigma_N^2, \end{aligned} \tag{8}$$

where we have assumed that $X_{k,n}$, $H_{k,n}$ and $N_p$ for all $k$, $n$ and $p$ are independent identically distributed (i.i.d.) random variables with zero means and variances of 1, $\sigma_{H,n}^2$ and $\sigma_N^2$, respectively. $S_p(x)$ has been defined as

$$S_p(x) \equiv \sum_{k=0,k\neq p}^{N-1} \left( \frac{\sin\left(\pi(k+x-p)\right)}{N\sin\left(\pi(k+x-p)/N\right)} \right)^2. \tag{9}$$

Appendix A shows that (9) is an even function, with the shape bulging downward on the interval $-1 \le x \le 1$ for all $p$. Using $-0.5 \le f_f^{(n)} \le 0.5$ for $n = 1, 2$, we also see that our objective function in (8) bulges downward on the interval $-0.5 \le f_c \le 0.5$ for all $p$, so that it attains a *unique* local minimal value. Thus, the compensation frequency that minimizes the objective function is obtained by differentiating (8) with respect to $f_c$ as

$$J_p'(f_c) = (-\sigma_{H,1}^2) S_p'(f_f^{(1)} - f_c) - \sigma_{H,2}^2 S_p'(f_f^{(2)} - f_c) \tag{10}$$

and finding the solution to satisfy $J_p'(f_c) = 0$, $-0.5 \le f_c \le 0.5$.

We obtain this solution separately for two MISO scenarios.

1) For the first scenario (referred to as "distributed #1") where both paths have nearly the same attenuation, i.e., $\sigma_{H,1}^2 = \sigma_{H,2}^2$, $J_p'(f_c) = 0$ for all $p$ when

$$f_c = \frac{f_f^{(1)} + f_f^{(2)}}{2}. \tag{11}$$

We can verify this by substituting (11) into (10) and by using the fact that $S_p'(x)$ is an odd function such as $S_p'(x) = -S_p'(-x)$ since the derivative of the even function becomes an odd function [19].

2) For the second scenario (referred to as "distributed #2") where two paths have different attenuations, i.e., $\sigma_{H,1}^2 \neq \sigma_{H,2}^2$, the solution satisfying $J_p'(f_c) = 0$ for all $p$ is

$$f_c \approx \frac{\sigma_{H,1}^2 f_f^{(1)} + \sigma_{H,2}^2 f_f^{(2)}}{\sigma_{H,1}^2 + \sigma_{H,2}^2}. \tag{12}$$

We can also verify this by substituting (12) in (10) and by using an odd function approximation such as $S_p'(x) \approx cx$ for small $x$, where $c$ is a constant. Geometrically speaking, (12) corresponds to a point that internally divides the line segment joining $f_f^{(1)}$ and $f_f^{(2)}$ in the ratio of $\sigma_{H,2}^2 : \sigma_{H,1}^2$.

Alternatively, we can set the power of the desired signal as an objective function:

$$\begin{aligned} \tilde{J}(f_c) &= E\left\{\left|X_{p,1}H_{p,1}\Lambda_{p,p}^{(1)} - X_{p+1,1}^{*}H_{p,2}\Lambda_{p,p}^{(2)}\right|^2\right\} \\ &= \sigma_{H,1}^2\tilde{S}(f_f^{(1)} - f_c) + \sigma_{H,2}^2\tilde{S}(f_f^{(2)} - f_c). \end{aligned} \tag{13}$$

In (13), $\tilde{S}(x)$ was defined as

$$\tilde{S}(x) \equiv \left(\frac{\sin(\pi x)}{N\sin(\pi x/N)}\right)^2, \tag{14}$$

which is an even function that is bulging upward on the interval $-1 \le x \le 1$ (see Appendix B). Using a similar method as above, we can see that the value maximizing (13) is identical to (11) and (12) for the two respective scenarios. Therefore, the compensation frequency in (11) and (12) is optimal in the sense of maximizing the desired signal power and minimizing the residual ICI-plus-noise power simultaneously.

## 3. Algorithm for Compensation Frequency Optimization in MISO-mode DVB-T2

In the derivation presented in the previous section, we assumed that perfect estimates of the dual CFOs $f_f^{(1)}$ and $f_f^{(2)}$ are given to the receiver. As mentioned before, simultaneously estimating the dual CFOs is an impossible task for DVB-T2. To obtain the estimates of dual CFOs, two transmitters should send P1 symbols alternately during two time slots. In other words, one transmitter sends a P1 symbol and estimates its own CFO during the P1 symbol decoding process, while the other is set to zero, i.e., a null P1 symbol. However, this decreases the data rate and is also practically infeasible for application to current systems. For this reason, the assumption of perfectly estimated dual CFOs can be unreasonable.

In this section, we propose an algorithm that finds the optimal compensation frequency without requiring estimates of dual CFOs. It adjusts the compensation frequency iteratively based on the measurement of the residual ICI-plus-noise power. To measure the residual ICI-plus-noise power, we use the conventional pilot-aided technique proposed in [20] that averages the square of the difference of the received noiseless pilot and its corresponding noisy one in the frequency domain. Since the residual ICI-plus-noise power depends on the compensation frequency, it can be expressed as a function of $f_c$:

$$I(f_c) = \frac{1}{|P|}\sum_{k\in P}\left(Y_k - (P_{k,1}\hat{H}_{k,1} + P_{k,2}\hat{H}_{k,2})\right)^2, \quad (15)$$

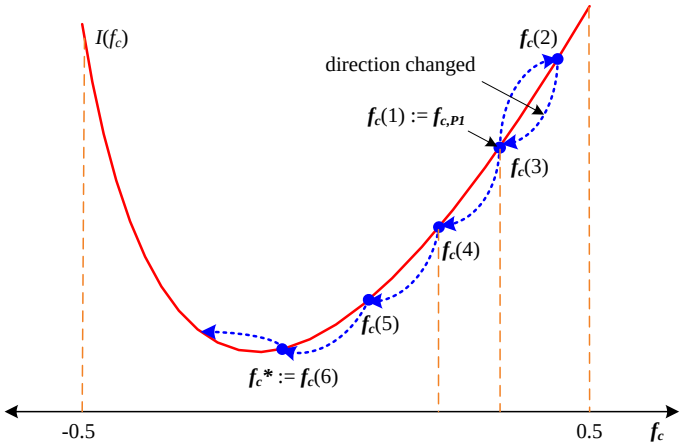


**Fig. 6.** Example of iterations of the proposed algorithm.

where $P_{k,n}$ and $\hat{H}_{k,n}$, $k\hat{\imath}\ \Pi$, $n$ = 1, 2, denote the pilot and estimate of the effective channel frequency response, respectively. Π is the set of pilot-bearing subcarriers, and |Π| is the number of elements in the set. Recall that the residual ICI-plus-noise power given in (8) is a function bulging downward on the interval $-0.5 \le f_c \le 0.5$. Hence, (15) has the same shape.

Using this property of the objective functions, the algorithm searches for the optimal compensation frequency directionally with a step size of Δ. **Fig. 6** illustrates an example of the algorithm. It starts with the initial compensation frequency $f_{c,p1}$, which is obtained by processing the sum of two concurrently received P1 symbols. After measuring the residual ICI-plus-noise power by using (15), it adjusts the compensation frequency by Δ. With the updated compensation frequency, it measures the residual ICI-plus-noise power by using (15) again. If the residual ICI-plus-noise power is larger than the previous one, the searching direction is changed to the opposite direction. It then repeats the procedures of adjusting the compensation frequency and measuring the residual ICI-plus-noise power iteratively until the residual ICI-plus-noise power is larger than the previous one. We describe the details of the algorithm more formally as follows, and its equivalent block diagram is shown in **Fig. 7-(b)**.

**Algorithm**: Search for Optimal Compensation Frequency

1: Set $k$ : = 0 and start with $f_c(0) := f_{c,p1}$ and $I(f_c(0))$
2: Set $f_c(k + 1) := f_c(k) + \Delta$
3: Compensate by $f_c(k + 1)$
4: Remove guard interval and perform FFT
5: Evaluate $I(f_c(k + 1))$
6: If $I(f_c(k + 1)) > I(f_c(k))$ and $k = 0$
then $\Delta := -\Delta$, $k := k + 1$, and go back to step 2
7: Else if $I(f_c(k + 1)) > I(f_c(k))$ and $k \neq 0$
then stop and $f_c^* := f_c(k)$
8: Otherwise, $k := k + 1$ and go back to step 2

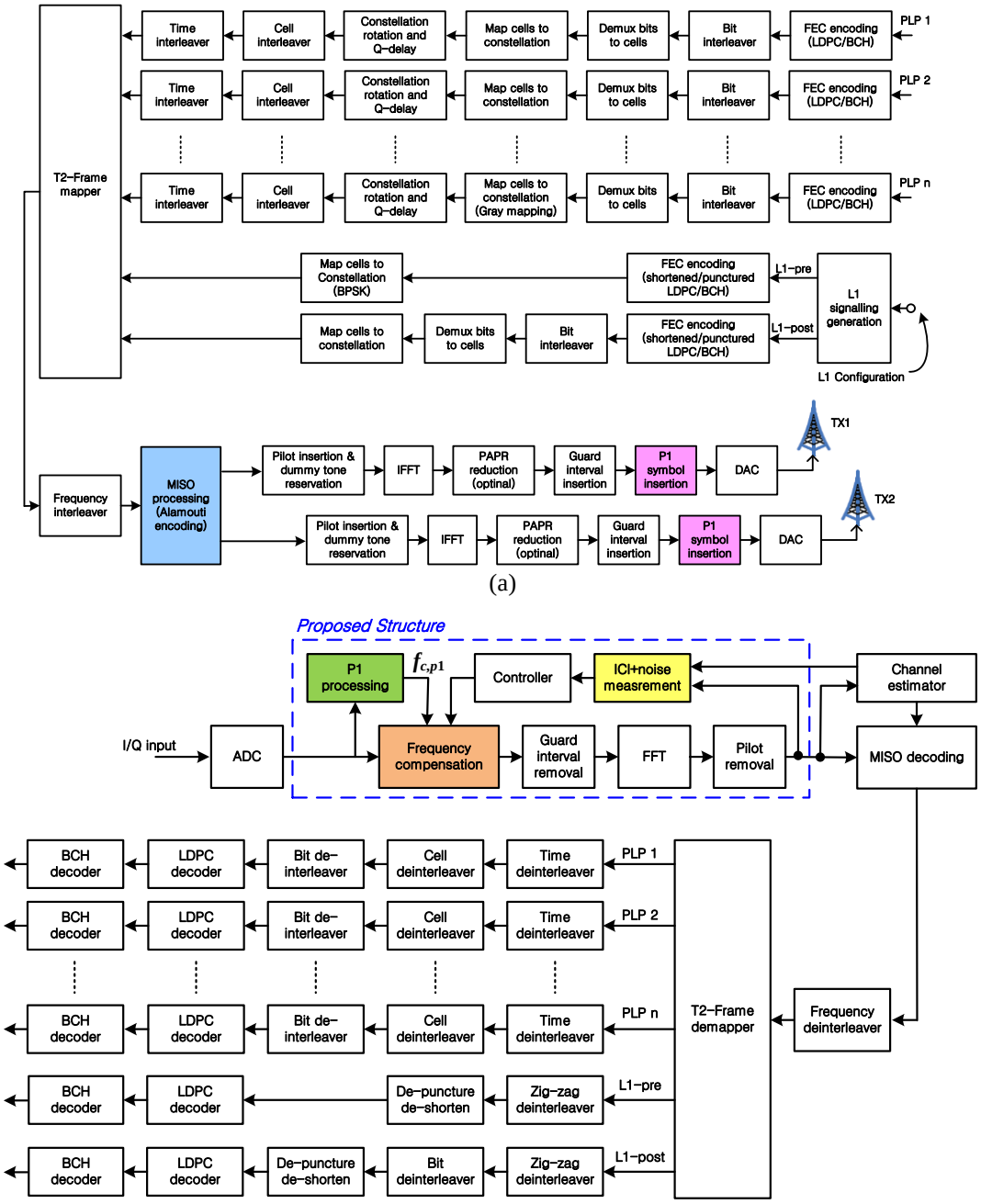


**Fig. 7.** Block diagram of DVB-T2: (a) MISO-mode transmitter, (b) receiver with proposed scheme.

## 4. Simulation Results

In this section, we validate the analytical results in Section 2 and present the performance evaluation of the proposed scheme in Section 3 via a full DVB-T2 simulator. The architecture of the DVB-T2 simulator is shown in **Fig. 7**, and the parameters are summarized in **Table 1**. The normalized CFOs for the two paths are set to 0.1 and 0.3, respectively. For the proposed

scheme, the step size for the normalized CFOs is chosen to be 0.01. To reduce the computational burden of repetitively processing guard interval removal, FFT, and the measurement of (15), the first P2 symbol containing 589 P2 pilots is employed for these processes. The MISO channel described in implementation guideline [2] is adopted for the channel model. The channel does not include any Doppler and should therefore be considered as a snapshot of the real time-variant channel. The channel frequency response $H_{k,n}$ is assumed to be known at the receiver. The MISO application scenario of distributed #1 is considered where $\sigma_{H,1}^2 = \sigma_{H,2}^2$. Thus, according to the results in Section 2, the optimal compensation frequency is the average value of the two CFOs, i.e., 0.2.

To verify this, **Fig. 8** illustrates the constellation of the received signal after channel compensation. To see only the effect of residual ICI, the effect of the AWGN is neglected. The modulation of the signal is quaternary phase-shift keying (QPSK). **Fig. 8-(a)** shows the case where the compensation frequency is set to one of the two CFOs (i.e., 0.1), while the case for optimal compensation frequency is shown in **Fig. 8-(b)**. These figures show that the effect of residual ICI is significantly reduced when the compensation frequency is set to the average

**Table 1.** DVB-T2 Simulation Parameters

| | Parameters | Options |
|---|---|---|
| OFDM | FFT size | 2K |
| | Pilot pattern | PP3 ($D_x$=6, $D_y$=4) |
| | Guard interval | 1/16 |
| | PAPR | No |
| | Carrier spacing | 4464Hz |
| | Frequency offset #1 (normalized value) | 446.4Hz (0.1) |
| | Frequency offset #2 (normalized value) | 1339Hz (0.3) |
| PLP | No. of PLPs | 1 |
| | PLP type | Common PLP |
| | Modulation | QPSK |
| | FEC rate | 1/2 (short frame) |
| | Constellation rotation | No |
| | Time interleaver type | Type 1 |
| L1 signal | Modulation (L1-pre) | BPSK |
| | FEC rate (L1-pre) | 1/4 (short frame) |
| | Modulation (L1-post) | QPSK |
| | FEC rate (L1-post) | 1/2 (short frame) |
| General | Bandwidth | 8MHz |
| | Carrier frequency | 730MHz (UHF Ch.) |
| | No. of LDPC iterations | 50 |
| | MISO channel type | Distributed #1 |
| | No. of T2 frames in a super frame | 2 |
| | No. of FEC blocks in a T2 frame | 5 |
| | No. of OFDM symbols in a T2 frame | 30 |
| | No. of AUX streams | 1 |
| | Bandwidth extension mode | No |

For a more detailed explanation on the parameters, please refer to [1].

**Table 2.** Average Iterations, Absolute Deviations and Required SNR to Achieve BER = $10^{-4}$ According to Different Step Sizes

| **Step Size(Δ)** | **0.05** | **0.01** | **0.005** | **0.001** |
|---|---|---|---|---|
| **Avg. iterations** | 4.808 | 7.973 | 12.063 | 44.602 |
| **Avg.** $\lvert f_{opt} - f_c^* \rvert$ | 0.01364 | 0.00593 | 0.00578 | 0.00559 |
| **Required SNR[dB] for BER = $10^{-4}$** | 2.8 | 2.68 | 2.68 | 2.68 |

value of the two rather than to one of the two. **Fig. 8-(b)** also shows that the constellations for both paths are separate from each other. As seen in the exponent of (6) in Section 2, the CFO introduces a phase shift in the desired signal that is proportional to the difference in each CFO and compensation frequency, i.e., $f_f^{(n)} - f_c$. Thus, when the compensation frequency is set to the average value of the two CFOs, the resultant signals are rotated in opposite directions, clockwise and counter-clockwise about the original QPSK constellation.

The reduction in residual ICI improves the BER performance. **Fig. 9** shows the BER performance of the PLP 1 data stream after low-density parity-check (LDPC) decoder. The compensation frequencies are set to [0.1, 0.15, 0.2 (optimal), 0.25, 0.3], respectively. This figure shows that the BER performance with optimal value are the best among all cases but had SNR loss of around 2 dB at a BER of $10^{-4}$ compared with CFO-free. This is due to the shifted phase and residual ICI as seen in **Fig. 8-(b)**. Furthermore, the cases for 0.15 and 0.25, which deviate from the optimal value by -0.05 and 0.05, respectively, have identical performance. The cases for 0.1 and 0.3, which deviate from the optimal value as -0.1 and 0.1, respectively, also have the same BER performance. However, the BER performances of the latter two cases are reduced compared with the former two. This implies that the BER performance is dependent upon the deviation from the optimal value and becomes worse as the gap increases.

**Fig. 10** compares the performance between the original MISO-mode T2 and T2 with proposed scheme. The original MISO-mode T2 system compensates the dual CFOs by using a CFO estimate from the P1 correlator that processes the sum of two simultaneously received P1 symbols, without adjustment. As seen in **Fig. 10**, the original T2 system results in significant performance loss and loses the waterfall shape in the BER curve. Thus, a higher SNR is needed for satisfactory HDTV reception that typically requires BER of less than $10^{-7}$ [2]. By contrast, the T2 with proposed scheme achieves the optimal performance and maintains the waterfall shape.

**Table 2** compares the average number of iterations, accuracy of compensation frequency in convergence $f_c^*$, and SNR required to achieve BER of $10^{-4}$ under different step sizes. The table shows that a large step size reduces the average number of iterations but increases the deviation from the optimal value $f_{\text{opt}}$. However, the BER performance is insensitive to the step size. Even with a large step size, the proposed algorithm achieved a near-optimal performance. Compared with the conventional scheme that needs about 4.5 dB for the same target BER, this is a noticeable gain. Thus, the proposed scheme is effective in terms of both efficiency and robustness.

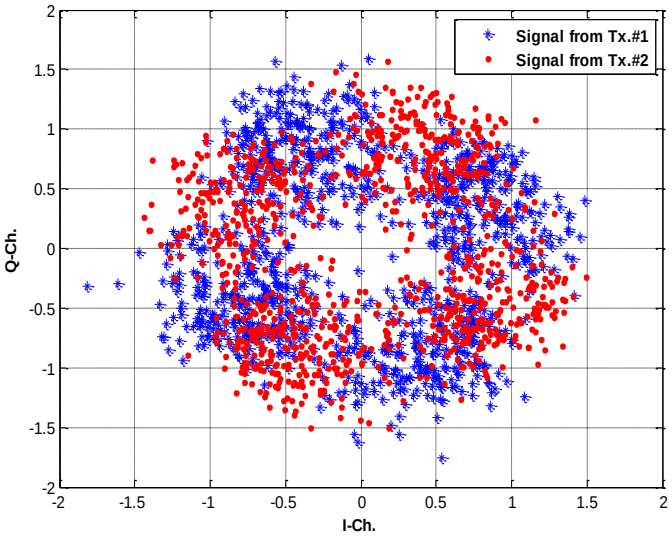


(a)

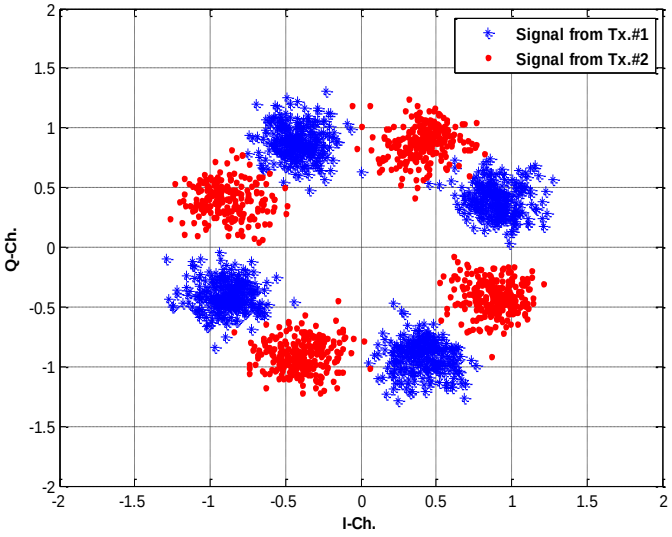


(b)

**Fig. 8.** Effect of compensation frequency on received constellation in the presence of dual CFOs $f_f^{(1)} = 0.1$ and $f_f^{(2)} = 0.3$, without AWGN noise:

(a) $f_c = 0.1$, (b) $f_c = 0.2$ (optimal).

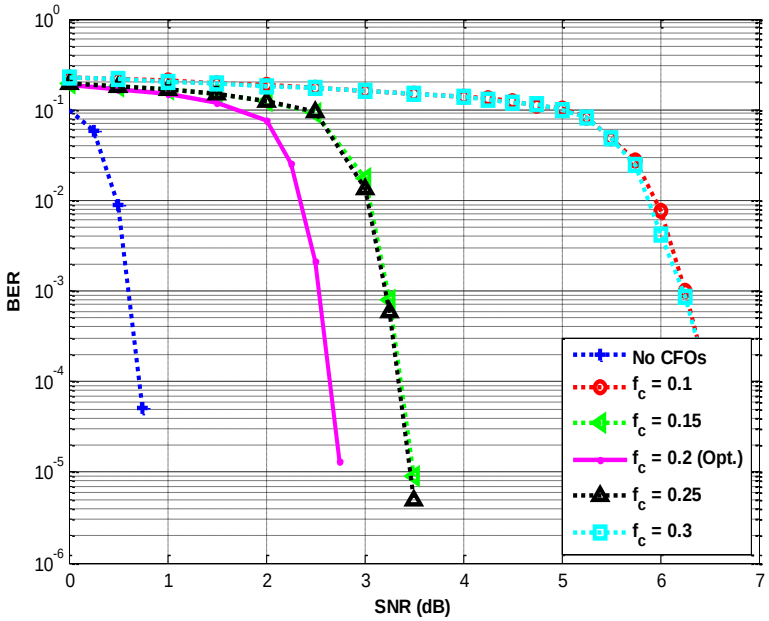


**Fig. 9.** Effect of compensation frequency on BER.

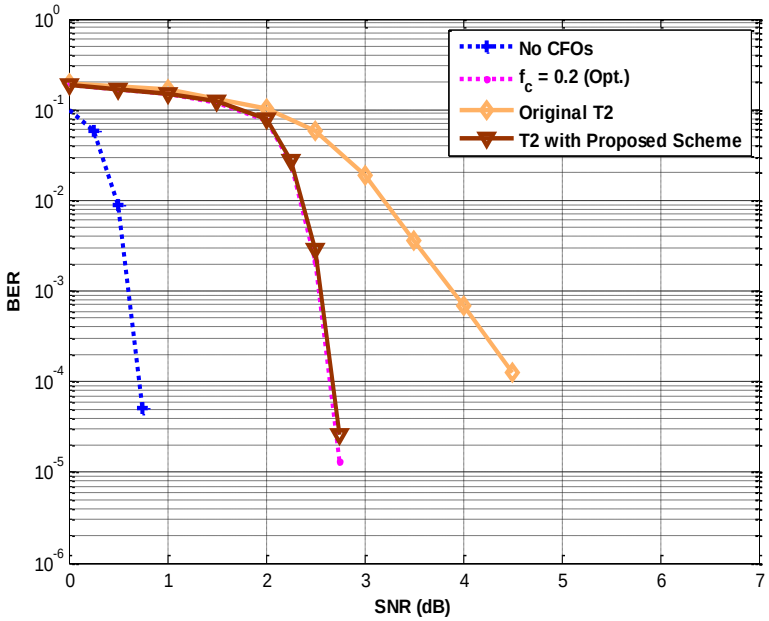


**Fig. 10**. BER comparison between the original T2 and T2 with proposed scheme.

## 5. Conclusion

In the presence of dual CFOs, residual ICI always exists after the CFO compensation is performed. In this paper, we theoretically have derived an optimal compensation frequency that minimizes the power of residual ICI-plus-noise under the assumption of perfectly estimated dual CFOs. For practical application to the MISO-mode DVB-T2, we have also proposed an algorithm that achieves the optimal compensation frequency without requiring estimates of dual CFOs. This iteratively adjusts the compensation frequency obtained from the P1 correlator based on the measurement of the residual ICI-plus-noise power. The simulation results validated the theoretical analysis and proved that utilizing the proposed scheme significantly reduces the degradation in BER performance resulting from the dual CFOs compared with the conventional one. The proposed scheme can be used in combination with existing ICI cancellation and equalization techniques such as those presented in [12][13][14][15][16][17][18] to further improve BER performance. Furthermore, the derived analytical result can be readily applied to any transmit-diversity OFDM system with dual CFOs.

## Appendix A: Property of (9)

*Lemma 1:* $S_p(x)$ in (9) has the following properties:

(a) $S_p(x)$ is equal for all $p$, i.e., $S_p(x) = S_0(x)$ for $p = 1, 2, \ldots, N - 1$.

(b) $S_p(x)$ is an even function about the origin, i.e., $S_p(x) = S_p(-x)$.

(c) The first derivative of $S_p(x)$ with respect to $x$ has an extreme value on the integer $i$, i.e., $S_p'(x)\big|_{x=i} = 0$.

(d) The second derivative of $S_p(x)$ with respect to $x$ is positive at the origin, i.e., $S_p''(x)\big|_{x=0} > 0$.

*Proof (a):*

$$S_p(x) = \sum_{k=0,k\neq p}^{N-1}\left(\frac{\sin(\pi(k+x-p))}{N\sin(\pi(k+x-p)/N)}\right)^2$$
$$= \underbrace{\sum_{k=0}^{p-1}\left(\frac{\sin(\pi(k+x-p))}{N\sin(\pi(k+x-p)/N)}\right)^2}_{A} + \underbrace{\sum_{k=p+1}^{N-1}\left(\frac{\sin(\pi(k+x-p))}{N\sin(\pi(k+x-p)/N)}\right)^2}_{B}. \quad \text{(A.1)}$$

Here,

$$A = \sum_{k=0}^{p-1}\left(\frac{\sin(\pi(k+x-p))}{N\sin(\pi(k+x-p)/N)}\right)^2$$
$$= \sum_{k=0}^{p-1}\left(\frac{\sin(\pi(k+x-p)+N\pi)}{N\sin(\pi(k+x-p)/N+\pi)}\right)^2 \quad \text{(A.2)}$$

$$= \sum_{a=N-p}^{N-1} \left( \frac{\sin(\pi(a+x))}{N \sin(\pi(a+x)/N)} \right)^2,$$

where $a = k + N - p$. In the second line, the fact that the square of the sine function is periodic with period $\pi$ is used.

$$\begin{aligned} B &= \sum_{k=p+1}^{N-1} \left( \frac{\sin(\pi(k+x-p))}{N \sin(\pi(k+x-p)/N)} \right)^2 \\ &= \sum_{b=1}^{N-p-1} \left( \frac{\sin(\pi(b+x))}{N \sin(\pi(b+x)/N)} \right)^2, \end{aligned} \tag{A.3}$$

where $b = k-p$. Therefore,

$$\begin{aligned} S_p(x) &= \sum_{a=N-p}^{N-1} \left( \frac{\sin(\pi(a+x))}{N \sin(\pi(a+x)/N)} \right)^2 + \sum_{b=1}^{N-p-1} \left( \frac{\sin(\pi(b+x))}{N \sin(\pi(b+x)/N)} \right)^2 \\ &= \sum_{k=1}^{N-1} \left( \frac{\sin(\pi(k+x))}{N \sin(\pi(k+x)/N)} \right)^2 \\ &= S_0(x). \end{aligned} \tag{A.4}$$

*Proof (b):* For simplicity, let us consider $p = 0$. Then,

$$\begin{aligned} S_0(x) &= \sum_{k=1}^{N-1} \left( \frac{\sin(\pi(k+x))}{N \sin(\pi(k+x)/N)} \right)^2 \\ &= \sum_{k=1}^{N-1} \left( \frac{\sin(\pi(k+x) - N\pi)}{N \sin(\pi(k+x)/N - \pi)} \right)^2 \\ &= \sum_{k=1}^{N-1} \left( \frac{\sin(\pi(N-k-x))}{N \sin(\pi(N-k-x)/N)} \right)^2 \\ &= S_0(-x). \end{aligned} \tag{A.5}$$

Since $S_p(x) = S_0(x)$ for $p = 1, 2, \cdots, N-1$ according to lemma 1(a), $S_p(x) = S_p(-x)$ for all $p$.

■

*Proof (c):* Taking the first derivative of (9) with respect to $x$ leads to

$$S_p'(x) = 2\sum_{k=0,k\neq p}^{N-1}\left(\frac{\sin(\pi(k+x-p))}{N\sin(\pi(k+x-p)/N)}\right) \tag{A.6}$$
$$\cdot\left(\frac{\pi\cos(\pi(k+x-p))N\sin(\pi(k+x-p)/N)}{(N\sin(\pi(k+x-p)/N))^2}+\frac{-\pi\cos(\pi(k+x-p)/N)\sin(\pi(k+x-p))}{(N\sin(\pi(k+x-p)/N))^2}\right).$$

From the first term in the summation, we can see that (A.6) becomes zero when $x$ is an integer value. This completes the proof.

■

*Proof (d):* After taking the second derivative of (9) with respective to $x$ and then substituting zero, we can obtain

$$S_p''(x)\Big|_{x=0} = \frac{\pi^2}{N^2\sin^2(\pi(k-p)/N)} > 0. \tag{A.7}$$

This completes the proof.

■

## Appendix B: Property of (14)

*Lemma2:* $\tilde{S}(x)$ in (14) has the following properties:

(a) $\tilde{S}(x)$ is an even function about the origin, i.e., $\tilde{S}(x) = \tilde{S}_p(x)$

(b) The first derivative $\tilde{S}_p(x)$ of has an extreme value on the integer $i$, i.e., $\tilde{S}'(x)\Big|_{x=i} = 0$.

(c) The second derivative of is negative at the origin, i.e., $\tilde{S}''(x)\Big|_{x=0} < 0$.

*Proof (a):* The proof is straightforward and omitted here.

*Proof (b):* After taking the first derivative of (14) with respective to $x$, we have

$$\tilde{S}'(x) = 2\frac{\sin(\pi x)}{N\sin(\pi x/N)}\cdot\left(\frac{\pi\cos(\pi x)N\sin(\pi x/N)-\pi\cos(\pi x/N)\sin(\pi x)}{N^2\sin^2(\pi x/N)}\right). \tag{A.8}$$

Applying l'Hospital's Rule [19], we see that the second term in (A.8) approaches 0 as $x \rightarrow i$.

■

*Proof (c):* After taking the second derivative of (14) with respective to $x$ and l'Hospital's

Rule, we can readily see that

$$\lim_{x\to 0}\tilde{S}''(x) = 2\left(1/N^2 - 1\right)\pi^2 . \tag{A.9}$$

Since $N = 2n$ and $n = 1, 2, ...$, (A.9) is negative. This completes the proof. ■

## References


[1] ETSI, "Digital video broadcasting (DVB): Framing structure, channel coding and modulation for a second generation digital terrestrial television broadcasting system (DVB-T2)," ETSI EN 302 755 V1.1.1, 2009. Article (CrossRefLink)

[2] ETSI, "Implementation guidelines for a second generation digital terrestrial television broadcasting system (DVB-T2)," DVB document A133, Nov.2009. Article (CrossRefLink)

[3] S. Alamouti, "A simple transmit diversity technique for wireless communications," *IEEE J. Sel. Areas in Commun.*, vol.16, no.8, pp.1451-1458, Oct.1998. Article (CrossRef Link)

[4] P. H. Moose, "A technique for orthogonal frequency division multiplexing frequency offset correction," *IEEE Trans. on Commun.*, vol.42, no.10, pp.2908-2914, Oct.1994. Article (CrossRefLink)

[5] J.-J. van de Beek, M. Sandell and P. O. Börjesson, "ML estimation of time and frequency offset in OFDM systems," *IEEE Trans. on Signal Process.*, vol.45, no.7, pp.1800-1805, Jul.1997. Article (CrossRefLink)

[6] M. Li and W. Zhang, "A novel method of carrier offset estimation for OFDM systems," *IEEE Trans. on Consumer Electron.*, vol.49, no.4, pp.965-972, Nov.2003. Article (CrossRefLink)

[7] M.-K. Oh, X. Ma, G. B. Giannakis and D.-J. Park, "Cooperative synchronization and channel estimation in wireless sensor networks," *Journal of Commun. and Networks*, vol.7, pp.284-293, Sep.2005. Article (CrossRefLink)

[8] Q. Huang, M. Ghogho, J. Wei, and P. Ciblat, "Practical timing and frequency synchronization for OFDM-based cooperative systems," *IEEE Trans. on Signal Process.*, vol. 58, no. 7, pp. 3706-3716, Jul. 2010. Article (CrossRefLink)

[9] Y. Yu, A. P. Petropulu, H. V. Poor, and V. Koivunen, "Blind estimation of multiple carrier frequency offsets," *in Proc. IEEE Int. Symp. on Personal, Indoor and Mobile Radio Commun. (PIMRC)*, Sep.2007. Article (CrossRefLink)

[10] Y. Yao and T.-S. Ng, "Correlation-based frequency offset estimation in MIMO system," *in Proc. of IEEE Vehicular Technol. Conf. (VTC-Fall)*, Oct.2003. Article (CrossRefLink)

[11] T.-H. Pham, A. Nallanathan, and Y.-C. Liang, "Joint channel and frequency offset estimation in distributed MIMO flat-fading channels," *IEEE Trans. on Wireless Commun.*, vol.7, no.2, pp.648-656, Feb.2008. Article (CrossRefLink)

[12] Z. Li, D. Qu and G. Zhu, "An equalization technique for distributed STBC-OFDM system with multiple carrier frequency offsets," *in Proc. of IEEE Wireless Commun. and Networking Conf. (WCNC)*, vol.2, pp.839-843, Apr.2006. Article (CrossRefLink)

[13] Y. J. Kim, H. Lee and H. K. Chung, and Y. S. Cho, "An iterative decoding technique for cooperative STBC-OFDM systems with multiple carrier frequency offsets," *in Proc. of IEEE Int. Symp. on Personal, Indoor and Mobile Radio Commun. (PIMRC)*, Sep.2007. Article (CrossRefLink)

[14] A. Ö. Yilmaz, "Cooperative diversity in carrier frequency offset," *IEEE Commun. Lett.*, vol.11, no.4, pp307-309, Apr.2007. Article (CrossRefLink)

[15] H. Wang, X.-G. Xia, and Q. Yin, "Distributed space-frequency codes for cooperative communication systems with multiple carrier frequency offsets," *IEEE Trans. on Wireless Commun.*, vol.8, no.2, pp.1045-1055, Feb.2009. Article (CrossRefLink)

[16] Q. Huang, M. Ghogho, D. Ma and J. Wei, "Low-complexity data-detection algorithm in cooperative SFBC-OFDM systems with multiple frequency offsets," *IEEE Trans. on Veh. Technol.*, vol.59, no.9, pp.4614-4620, Nov.2010. Article (CrossRefLink)

[17] K. H. Kim, S. W. Kang, M. Mohaisen and K. H. Chang, "An algorithm for iterative detection and decoding MIMO-OFDM HARQ with antenna scheduling," *KSII Trans. on Internet and Inf. Syst.*, vol.2, no.4, Aug.2008. Article (CrossRefLink)
[18] M. Mohaisen, H. An and K.-H. Chang, "Detection techniques for MIMO multiplexing: a comparative review," *KSII Trans. on Internet and Inf. Syst.*, vol.3, no.6, Dec.2009. Article (CrossRefLink)
[19] J. Stewart, *Calculus: Early Transcendentals*, Thomson Brooks/Cole, CA, USA, 6th edition, 2008.
[20] S. He and M. Torkelson, "Effective SNR estimation in OFDM system simulation," *in Proc. of IEEE Global Telecommun. Conf. (GLOBECOM)*, vol.2, pp.945-950, Nov.1998. Article (CrossRefLink)

**Eun-Sung Jeon** received his B.S. (honors) and M.S. degrees in Electrical and Electronics Engineering from Yonsei University, Seoul, Korea, in 2005 and 2007 respectively. Since 2007, he has been in the Ph.D. program of Electrical and Electronic Engineering at Yonsei University. His main research interests include signal processing techniques for communication and broadcasting systems.

**Jeong-Wook Seo** received his B.S. and M.S. degrees in the Department of Telecommunication and Information Engineering from Korea Aerospace University, Gyeonggi, Korea, in 1999 and 2001, respectively and his Ph.D. in the Department of Electrical and Electronic Engineering from Yonsei University, Seoul, Korea in 2010. Since 2001, he has been with Advanced Mobile Technology Research Center in Korea Electronics Technology Institute (KETI), Gyeonggi, Korea. His research interests include statistical signal processing, digital communications, and OFDM-based wireless systems.

**Jang-Hoon Yang** received his Ph.D. in Electrical Engineering from University of Southern California, Los Angeles, USA, in 2001. He is currently an Assistant Professor at the Department of Newmedia, Korean German Institute of Technology, Seoul, Korea. From 2001 to 2006, he was with communication R&D center, Samsung Electronics. From 2006 to 2009, he was a Research Assistant Professor at the Department of Electrical and Electronic Engineering, Yonsei University. He has published numerous papers in the area of multi-antenna transmission and signal processing. His research interest includes wireless system and network, artificial intelligence, neuroscience, and brain computer interface.

**Richard (Jong-Ho) Paik** received the B.S., M.S., and Ph.D. degrees in the school of Electrical and Electronic Engineering from Chung-Ang University, Seoul, Korea, in 1994, 1997, and 2007, respectively. He was a Director with Advanced Mobile Research Center at Korea Electronics Technology Institute (KETI) by 2011. He is currently a assistant professor in the Multimedia department, Seoul Women's University, Seoul, since 2011. His research interests are in the areas of wireless/wired communications system design, video communications system design, and system architecture for realizing advanced digital communications system and for advanced mobile broadcasting networks as well.

**Dong-Ku Kim** received his B.S. degree from the Korea Aerospace University in 1983, and his M.S. and Ph.D. degrees from the University of Southern California, Los Angeles, in 1985 and 1992, respectively. He worked on CDMA systems in the cellular infrastructure group of Motorola, Fort Worth, TX, in 1992. He has been a Professor in the Department of Electrical and Electronic Engineering, Yonsei University, Seoul, Korea, since 1994, and was also a director of Radio Communication Research Center, Yonsei University. His research interests are cooperative MIMO and relays, interference management, compressive sensing for device to device communication, and UAV tracking.